# Antitumor Effect of 2-Methoxyestradiol in a Rat Orthotopic Brain Tumor Model

Seung-Hee Kang,[1,7] Heidi T. Cho,[1] Sarojini Devi,[2] Zhaobin Zhang,[2] Daniel Escuin,[6] Zhongxing Liang,[1] Hui Mao,[3] Daniel J. Brat,[4] Jeffrey J. Olson,[2] Jonathan W. Simons,[1,5] Theresa M. LaVallee,[8] Paraskevi Giannakakou,[6] Erwin G. Van Meir,[1,2,5] and Hyunsuk Shim[1,3,5]

Departments of [1]Hematology/Oncology, [2]Neurosurgery, [3]Radiology, and [4]Pathology and [5]Winship Cancer Institute, Emory University, School of Medicine, Atlanta, Georgia; [6]Department of Hematology/Oncology, Weill Cornell Medical College of Cornell University, New York, New York; [7]Department of Radiation Oncology, Ajou University Hospital, Suwon, Korea; and [8]EntreMed, Inc., Rockville, Maryland

## Abstract

**Grade 4 malignant glioma (GBM) is a fatal disease despite aggressive surgical and adjuvant therapies. The hallmark of GBM tumors is the presence of pseudopalisading necrosis and microvascular proliferation. These tumor cells are hypoxic and express hypoxia-inducible factor-1 (HIF-1), a prosurvival transcription factor that promotes formation of neovasculature through activation of target genes, such as *vascular endothelial growth factor*. Here, we evaluated whether 2-methoxyestradiol, a microtubule and HIF-1 inhibitor, would have therapeutic potential for this disease in a 9L rat orthotopic gliosarcoma model using a combination of noninvasive imaging methods: magnetic resonance imaging to measure the tumor volume and bioluminescence imaging for HIF-1 activity. After imaging, histologic data were subsequently evaluated to elucidate the drug action mechanism *in vivo*. Treatment with 2-methoxyestradiol (60–600 mg/kg/d) resulted in a dose-dependent inhibition of tumor growth. This effect was also associated with improved tumor oxygenation as assessed by pimonidazole staining, decreased HIF-1α protein levels, and microtubule destabilization as assessed by deacetylation. Our results indicate that 2-methoxyestradiol may be a promising chemotherapeutic agent for the treatment of malignant gliomas, with significant growth inhibition. Further studies are needed to assess the effect of low or intermediate doses of 2-methoxyestradiol in combination with chemotherapeutic agents in clinical studies focused on malignant gliomas. In addition to showing tumor growth inhibition, we identified three potential surrogate biomarkers to determine the efficacy of 2-methoxyestradiol therapy: decreased HIF-1α levels, α-tubulin acetylation, and degree of hypoxia as determined by pimonidazole staining.** (Cancer Res 2006; 66(24): 11991-7)

## Introduction

Malignant glioma (GBM) is the most common primary brain tumor and is uniformly fatal despite aggressive surgical and adjuvant therapies. Current therapeutic efficacy is limited by both acquired and inherent tumor resistance, which can be attributed to the blood-brain barrier (BBB), tumor hypoxia, and a relatively slow growth rate. Thus, identification of new agents directed against novel cellular targets in GBM would be beneficial.

One characteristic feature of GBM is the presence of hypoxic areas associated with increased angiogenesis. Hypoxia-inducible factor-1 (HIF-1) regulates the expression of target genes critical for the formation of new vasculature and provides a plausible explanation for the vascular hyperplasia seen in GBM (1, 2). This prosurvival transcription factor is involved in the response of both normal and tumor cells to hypoxia and consists of two subunits: HIF-1α and HIF-1β. The HIF-1α subunit is rapidly degraded under normoxic conditions, whereas the HIF-1β subunit is constitutively expressed. Under hypoxic conditions, HIF-1α is stabilized and dimerizes with HIF-1β to form an active transcription factor. The dimer then binds to the DNA sequence 5′-RCGTG-3′ [hypoxia-responsive element (HRE)], located in the promoter of target genes. This subsequently leads to up-regulation of factors that promote tumor growth and angiogenesis, including glycolytic enzymes and vascular endothelial growth factor (VEGF; refs. 3, 4). These data suggest that HIF-1 is a promising new target for the treatment of GBM.

HIF-1 transcriptionally up-regulates VEGF production as part of the oxygen regulation system that stimulates the production of new blood vessels to support tumor growth (5). Overexpressed VEGF leads to increased capillary leakiness and vascular permeability, which is followed by vascular hyperplasia, leading to increased vessel density. Therefore, high expression of VEGF in tumor tissues is a strong indicator of poor treatment response. Among the most promising new therapies coming to clinical trials for GBM are antiangiogenic therapies and treatments targeting HIF-1α.

2-Methoxyestradiol is a naturally occurring estrogen metabolite that exhibits antiproliferative and antiangiogenic activity by inducing apoptosis as well as inhibiting HIF-1α, microtubules, and tumor angiogenesis (6–9). 2-Methoxyestradiol binds directly to the colchicine binding site of the tubulin protein, thereby inhibiting polymerization (10). This disruption not only interferes with the mitotic spindle apparatus but also inhibits HIF-1α translation and its nuclear translocation (6, 11). Mabjeesh et al. (6) reported that 2-methoxyestradiol down-regulated HIF-1α, downstream of microtubule disruption, by inhibiting its *de novo* synthesis. 2-Methoxyestradiol was also shown to preferentially kill tumor cells over normal cells by causing reactive oxygen species (ROS) accumulation in cancer cells (12). Pelicano et al. further reported that inhibition of the mitochondrial electron transport chain by arsenic trioxide, an antineoplastic medicine, enhanced ROS generation and

**Competing interest statement:** T.M. LaVallee is an employee of EntreMed, Inc.
**Requests for reprints:** Hyunsuk Shim, Winship Cancer Institute, 1701 Uppergate Drive, C5008, Atlanta, GA 30322. Phone: 404-778-4564; Fax: 404-778-5550; E-mail: hyunsuk.shim@emory.org.

doi:10.1158/0008-5472.CAN-06-1320

increased its anticancer effect when combined with 2-methoxyestradiol (13).

Panzem (EntreMed, Inc., Rockville, MD), or 2-methoxyestradiol, is currently in phase I/II clinical studies to investigate its safety, efficacy, and pharmacokinetics. Studies with xenograft and metastatic cancer animal models indicate that 2-methoxyestradiol targets both the tumor and the tumor vasculature in sarcomas and melanomas (14). Because of the prominent vasculature of GBM and the dependence on angiogenesis for malignant progression, it is of great interest to investigate the potential therapeutic effects of Panzem for GBM. Here, we evaluate the efficacy and mechanisms of Panzem in the 9L rat orthotopic glioma model using a combination of noninvasive imaging methods [magnetic resonance imaging (MRI) and bioluminescence imaging (BLI)] to measure tumor volume and histology at termination.

## Materials and Methods

### Cell Line and Growth Conditions

9L rat glioma cells were grown in DMEM medium (Invitrogen, Carlsbad, CA) supplemented with 10% fetal bovine serum (Sigma, St. Louis, MO) and antibiotics at 37°C in 5% $CO_2$. To generate 9L cells reporting HIF-1 activity, we stably cotransfected 9L rat glioma cells with a luciferase expression vector (V6R) to monitor HIF-1 activity and pCDNA3.1 for drug selection (mixture ratio of luciferase vector/pCDNA 3.1 = 5:1) using LipofectAMINE 2000 (Invitrogen). The V6R HIF-1 reporter plasmid contains a firefly luciferase gene whose expression is driven by six tandem copies of the HRE derived from the *VEGF* gene promoter (15). Single-cell G418-resistant clones showing elevated luciferase activity under hypoxic conditions were selected. Five clones showing the greatest increase in luciferase activity in response to hypoxia were pooled and used in animal experiments.

### *In vitro* Cell Growth Inhibition

2-Methoxyestradiol (EntreMed) was dissolved in DMSO to obtain a 30 mmol/L stock solution. 9L cells were plated in 60-mm tissue culture Petri dishes in complete medium. Cells were then treated the following day with fresh medium containing 2-methoxyestradiol at concentrations of 10 or 50 μmol/L and then incubated for 48 hours. Cell growth was assessed by counting cells using a hemacytometer. All experiments were done in quadruplicate. In the hypoxic experiment, 9L cells in 60-mm Petri dishes were transferred to the Invivo2 Hypoxia Workstation 1000 (Biotrace, Bothell, WA) immediately after seeding. The cells were treated with 2-methoxyestradiol concentrations of 0 μmol/L (control), 10 μmol/L, or 50 μmol/L 24 hours after seeding. Two humidified hypoxic tissue culture incubators were maintained with an atmospheric pressure of either 1% $O_2$ or 5% $O_2$ with 5% $CO_2$ in nitrogen gas. Forty-eight hours following 2-methoxyestradiol treatment, the Petri dishes were removed from the hypoxic incubator and trypsinized for cell counting.

### Implant of Tumor Cells to Rat Brain

We stereotactically injected 9L-V6R cells (50,000 in 5 μL volume) into the brains of Fischer 344 rats (average body weight = 150 g) as reported by Barker et al. (16) at stereotactic coordinates 1 mm forward of the frontal zero plane, 3 mm to the right of midline, and 4.5 mm deep.

### 2-Methoxyestradiol Treatment

For *in vivo* experiments, Panzem (nanocrystal colloidal dispersion; Elan Drug Delivery, King of Prussia, PA) was used. Rats ($n$ = 6 per group) were treated with an i.p. injection of the vehicle (60, 200, or 600 mg/kg/d of 2-methoxyestradiol/Panzem) for nine consecutive days beginning on the 8th day after the initial tumor cell injection. The experiment was repeated a second time using three rats per group.

### Imaging Studies

***BLI.*** Seven days after the tumor cell injection, the viable hypoxic tumor was identified by noninvasive BLI (Xenogen, Alameda, CA). BLIs were obtained using a Xenogen Small Animal Imager (IVIS Imaging System) equipped with Living Image software. Eight days after the tumor cell injection and before initiation of treatment, rats were anesthetized by i.p. injection of a ketamine (80 mg/kg)/xylazine (4 mg/kg) mixture. Rats were then injected with luciferin (100 mg/kg of luciferin; Xenogen) i.p., and after 15 minutes of incubation, 1-minute image acquisition at medium binning was taken. Imaging by BLI was also done on the 9th day of treatment.

***MRI.*** The response to 2-methoxyestradiol treatment was assessed by the measurement of tumor volume using noninvasive MRI before and after the treatment. Brain images of each animal were obtained on the first day of the treatment (4 hours after BLI to allow animals to recover) and on the 8th day of the treatment. The MRI scan was carried out using a 3T MRI scanner (Philips Intera) and a small volume coil (5-cm diameter). The animals were anesthetized by an i.p. injection of a ketamine (80 mg/kg)/xylazine (4 mg/kg) mixture and then placed in the coil. The head was secured using foam padding to minimize possible movements. Each animal received 1.0 ml/kg (0.2 mmol/L/kg) of Gadolinium diethylenetriaminepentaacetic acid (Gd-DTPA) i.v. A set of multi-slice, $T_1$-weighted, spin echo images were obtained in the coronal section by using a repetition time of 400 ms, an echo time of 14 ms, and an imaging matrix of 128 × 128 with a field of view of 50 × 50 $mm^2$. To match histologic analysis, a slice thickness of 2 mm was used without a slice gap. The number of signal averages was three for the majority of the scans. Tumors shown in the MRI were measured in three orthogonal dimensions. Tumor volume ($V$) was calculated as: $V$ ($mm^3$) = $\pi(a \times b \times c) / 6$, where $a$, $b$, and $c$ represent width, height, and thickness, respectively. The mean rat brain volume was about 550 to 600 $mm^3$, which was consistent with the size reported by Sahin et al. (17) using histologic measurements of rat brain sections. A mean of these individual values was used. Following the MRI scans, rats were grouped to obtain an even distribution of tumor sizes.

All protocols for animal studies were reviewed and approved by the Institutional Animal Care and Use Committee at Emory University.

### Immunohistochemistry

Pimonidazole is used to delineate the hypoxic site of the tumors due to its specific binding to cells in a partial oxygen tension <10 mm Hg. We injected animals with pimonidazole hydrochloride (hydroxyprobe-1; Chemicon, Temecula, CA) i.p. (60 mg/kg) 90 minutes before the animals were sacrificed. Upon sacrifice of the animal, the entire brain was collected and briefly fixed in 10% neutral buffered formalin for 5 minutes. The harvested rat brain was then placed in a formalin bath with an acrylic brain matrix (Ted Pella, Inc., Redding, CA) and immobilized using two razor blades. The isolated brain was sliced into 2-mm thickness from the tip of the frontal lobe to the end of occipital lobe to match the coronal sections of the MRI. Each slice was placed with the frontal part facing down in the uni-cassettes (Tissue-Tek, Fisher Scientific, Hampton, NH) before embedding in paraffin. The intersection of the septum pellucidum and the corpus callosum was used as a focal point to match histology with MRI. Several 6-μm-thick slices were sectioned from each paraffin-embedded block, and one slice from each block was stained with H&E to match the MRI data. The selected tissue sections were subjected to immunohistochemical staining using antibodies against pimonidazole (hypoxyprobe-1; Chemicon), HIF-1α (Novus Biologicals, Littleton, CO), and acetylated α-tubulin (Sigma, St. Louis, MO).

To visualize pimonidazole staining, deparaffinized sections were immunostained with a hypoxyprobe-1 antibody following manufacturer instructions (Chemicon). Images were acquired with a Nikon Eclipse E800 microscope.

The detailed procedure of HIF-1α immunostaining was described previously (18), and similar procedures were used for acetylated α-tubulin immunostaining (anti–acetylated α-tubulin antibody, 1 μg/mL).

For quantitative analysis of immunohistochemical results, two to four representative pictures were acquired from each slide using a Zeiss Axioskop microscope equipped with a Sony CCD video camera system. Images were collected at magnifications of ×400 for HIF-1α and acetylated α-tubulin and ×100 for pimonidazole. The overall degree of positive staining, as indicated by the brown color, was semiquantitatively estimated

with four grades (−, +, ++, and +++) by three different people (S.K., D.J.B., and H.S.). Grids were placed on the captured images, and the entire area of the picture, excluding the non-tumor area, was counted. Additionally, an immunostaining score was calculated by the multiplication of the percentage of positive tumor cells (0–100%) and the staining intensity (grades 1–4), producing a total range of 0 to 4 (19).

## Results

**2-Methoxyestradiol effect on 9L cells *in vitro*.** To assess the effect of 2-methoxyestradiol on *in vitro* cell growth, 9L cells grown in complete medium were exposed to two different concentrations (10 or 50 μmol/L) of 2-methoxyestradiol for 48 hours. 9L cells were relatively resistant to 2-methoxyestradiol compared with other glioma cell lines with <50% inhibition observed after 48 hours of treatment in normoxia (Fig. 1) at concentrations up to 50 μmol/L. However, 9L cells became more sensitive to 2-methoxyestradiol as the oxygen tension decreased. 9L cells also proliferated at a slower rate in lower oxygen conditions than in normoxia. Unlike other chemotherapeutic agents or radiation therapy that are more effective on quickly growing, normoxic cells than slowly growing, hypoxic cells, 2-methoxyestradiol seems to affect slowly growing cells in hypoxia more than the normoxia counterpart. We recognize that the 9L tumor cells do not precisely represent human glioblastomas because of tumor homogeneity, lack of invasive nature, and more rapid growth rate. However, its reliability and ability to reside successfully in the brain allows it to be used as an initial approximation of human brain tumors. In a separate study, the treatment of other human glioma cell lines (U87MG and LN229) with 2-methoxyestradiol resulted in varying $IC_{50}$s of 10 and 5 μmol/L, respectively, in normoxia, indicating differences in cell line sensitivity to 2-methoxyestradiol.

**Monitoring the inhibition of 2-methoxyestradiol on tumor growth by MRI and its anti-HIF-1 activity by BLI.** 2-Methoxyestradiol has been previously shown to reduce HIF-1α synthesis through disruption of microtubule function *in vitro* (6), whereas 2-methoxyestradiol-induced HIF-1 inhibition *in vivo* has never been shown before. To study the relation between 2-methoxyestradiol and its effect on HIF-1 function *in vivo*, we generated a 9L rat glioma cell line (9L-V6R) stably transfected with a HIF-responsive luciferase expression vector (V6R). These cells were injected orthotopically, allowing for detection of HIF-1 activity in tumor cells by noninvasive BLI.

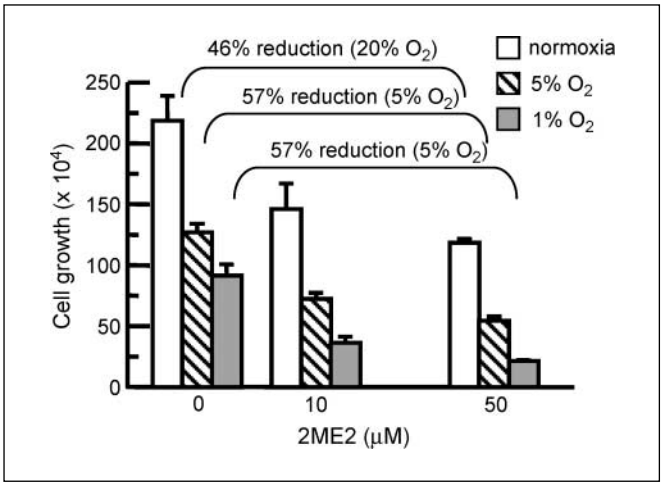


**Figure 1.** Treatment of 9L rat glioma cells with 2-methoxyestradiol (*2ME2*) at different oxygen concentration. 9L cells were seeded in 60-mm Petri dish in quadruplicate per concentration of drug treated. Two different concentrations of 2-methoxyestradiol were tested: 50 and 10 μmol/L and a control. Cell numbers were counted 48 hours after treatment to determine growth inhibition ($P$ = 6.8e-6, 3.6e-6, and 1.3e-6 for the untreated control versus 50 μmol/L group at normoxia, 5%, and 1% oxygen concentrations, respectively).

Four groups of rats were treated with an i.p. injection of the vehicle (60, 200, or 600 mg/kg/d of 2-methoxyestradiol/Panzem) for nine consecutive days beginning on the 8th day after the initial tumor cell injection. Tumor size and localization were determined by $T_1$-weighted contrast-enhanced (Gd-DTPA) MRI. Representative coronal MRI images from each group, before and after treatment, showed significant dose-dependent growth inhibition as a result of 2-methoxyestradiol treatment (Fig. 2*A*). Changes in tumor volume were determined by comparing MRI images obtained before the start of therapy (day 8 after tumor cell implantation) with those obtained on the 9th day of treatment for each dose of 2-methoxyestradiol and the vehicle control ($n$ = 6 for each group). There were minor variations in initial tumor volume before the treatment; however, these variations among the groups were not statistically significant. Tumor volumes at the end of treatment were 283.25 ± 49.87, 70.21 ± 36.12, 56.81 ± 26.80, and 12.61 ± 8.03 $mm^3$ for 0, 60, 200, and 600 mg/kg/d, respectively ($n$ = 6; $P$ = 0.0194, $P$ = 0.00204, $P$ = 0.0147 for the 60 versus 200 mg/kg/d, the 60 versus 600 mg/kg/d, and the 200 versus 600 mg/kg/d groups, respectively). Tumor volumes for individual animals before and after 2-methoxyestradiol treatment are shown in Fig. 2*B*. Even at the lowest dose tested (60 mg/kg/d), tumor volume was significantly reduced (4-fold reduction, $P$ = 0.00596) compared with the control animals; at the highest dose (600 mg/kg/d), there was an even greater reduction in tumor volume (23-fold reduction, $P$ = 0.0509). Some drug related toxicity was observed at 600 mg/kg/d dose, which was most frequently seen as diarrhea and weight loss (12–15%) and the death of one animal. These MRI data showed that tumor growth was blocked by 2-methoxyestradiol treatment in a dose-dependent manner.

Further validation of the noninvasive imaging-based measurement of the tumors was achieved by generating 2-mm tissue sections that were aligned with the MRI data (also obtained with a slice thickness of 2 mm). H&E staining was done on 6-μm sections from each paraffin block. Tumor shape and location in H&E-stained sections correlated well with the MRI images (Fig. 2*C*). This analysis validated the tumor volume measurement by MRI and confirmed that 2-methoxyestradiol treatment resulted in a dose-dependent inhibition of tumor growth.

The effect of 2-methoxyestradiol on HIF-1 activity was determined using BLI. Figure 3 shows that 2-methoxyestradiol treatment, particularly at the highest dose, dramatically decreased HIF-1 transcriptional activity. At low and intermediate doses, HIF-1 transcriptional activity measured by BLI was comparable with the tumor volume reduction determined by MRI. In other words, the relative HIF-1 activity measured by BLI over tumor volume measured by MRI was not significantly reduced. Thus, it seemed that 2-methoxyestradiol treatment did not appreciably affect HIF-1 transcriptional activity at the 60 or 200 mg/kg/d doses based on BLI data alone.

**Immunohistochemical analysis of 2-methoxyestradiol effects.** The *in vivo* HIF-1 activity in viable tumors from treated and control animals, as determined by BLI, was related to the presence of hypoxic areas in tissue sections using immunohistochemistry for HIF-1α protein and the hypoxic marker pimonidazole.

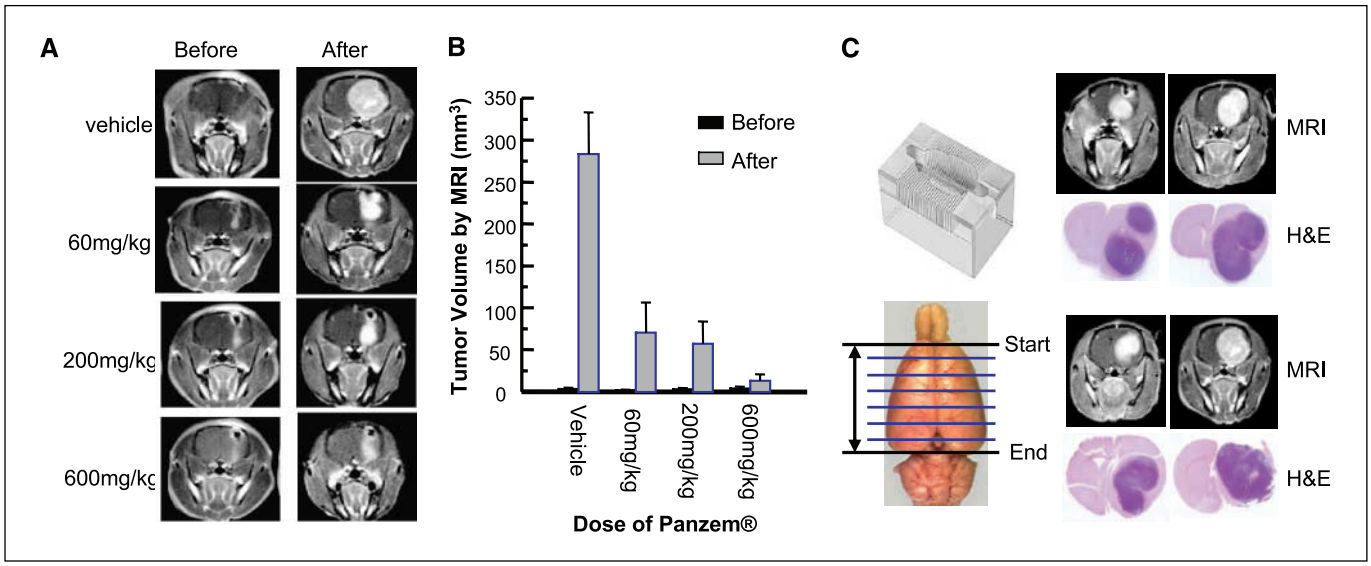


**Figure 2.** *A,* a representative Gd-DTPA enhanced $T_1$-weighted MRI image from each treatment group: *left,* before treatment; *right,* after treatment. *B,* summary of the tumor volume from the six rats in each group; all 24 rats before and after 2-methoxyestradiol treatment were measured by noninvasive post-contrast $T_1$-weighted MRI ($P$ = 7.1e−6, 1.9e−6, and 8.3e−7 for the control versus 60, 200, and 600 mg/kg/d groups, respectively). *C, top left,* acrylic brain matrices used to slice the rat brain into a 2-mm thickness from the tip of the frontal lobe of cerebrum (*Start*) to match with the MRI data that were scanned in the same orientation (*End*; *bottom left*). Each slice was placed with the frontal part, facing down, into uni-cassettes and paraffin embedded. H&E-stained tissue sections from paraffin-embedded blocks were lined up with their counterpart MRI images, which verified a reasonable correlation between tumor volume determined by MRI and histologic findings (*right*).

The harvested rat brain was processed as described in the legend of Fig. 2*C* to match the coronal sections of the MRI.

Figure 4 shows immunohistochemical staining of HIF-1α (*A*) and pimonidazole (*B*) of one representative tumor tissue per group. The tumor tissue from the control group was strongly HIF-1α positive, whereas the tumor tissues from the 60, 200, and 600 mg/kg/d groups showed reduced staining for HIF-1α as summarized in Table 1. The percentage of cells with strong HIF-1α-positive staining (+++) was significantly decreased to 24.0%, 18.2%, and 12.0% for 60, 200, and 600 mg/kg/d, respectively, compared with the vehicle-treated group (35.5%). Thus, 2-methoxyestradiol treatment reduced the gross HIF-1α protein levels in a dose-dependent manner (Fig. 4*A*; Table 1). HIF-1α staining results at the highest dosage (600 mg/kg/d) correlated well with BLI results. However, anti-HIF1 activity of 2-methoxyestradiol determined by immunohistochemistry contradicted BLI results at intermediate doses (60 or 200 mg/kg/d).

We further examined the effect of 2-methoxyestradiol on the tumor microenvironment by pimonidazole staining (Fig. 4*B*), which identifies viable hypoxic tumor cells, regardless of HIF-1α status (20–23). In agreement with HIF-1α immunostaining, tumor tissues from all three treated groups exhibited weaker pimonidazole staining than the control tissues, as summarized in Table 1. The percentage of cells with strong pimonidazole-positive staining (+++) was significantly decreased in the 2-methoxyestradiol-treated group (36.0% for 60 mg/kg/d and 0% for 200 and 600 mg/kg/d) compared with the vehicle-treated group (86.5%). This may be attributed to the dramatic inhibition of tumor growth in a dose-dependent manner following 2-methoxyestradiol treatment.

Escuin et al. have shown that inhibition of HIF-1 activity by 2-methoxyestradiol requires disruption of microtubules (24). To determine if the antitumor and HIF-1 inhibition observed *in vivo* could be correlated with the 2-methoxyestradiol effect on the microtubules of the tumor cells, we analyzed the levels of acetylated α-tubulin. Most α-tubulins are known to be post-translationally modified by acetylation on the epsilon-amino group of a lysine residue in the $NH_2$ terminus (25). Acetylation is associated with more stable and mature microtubules (26); hence, drugs that hyperstabilize microtubules, such as taxanes, enhance

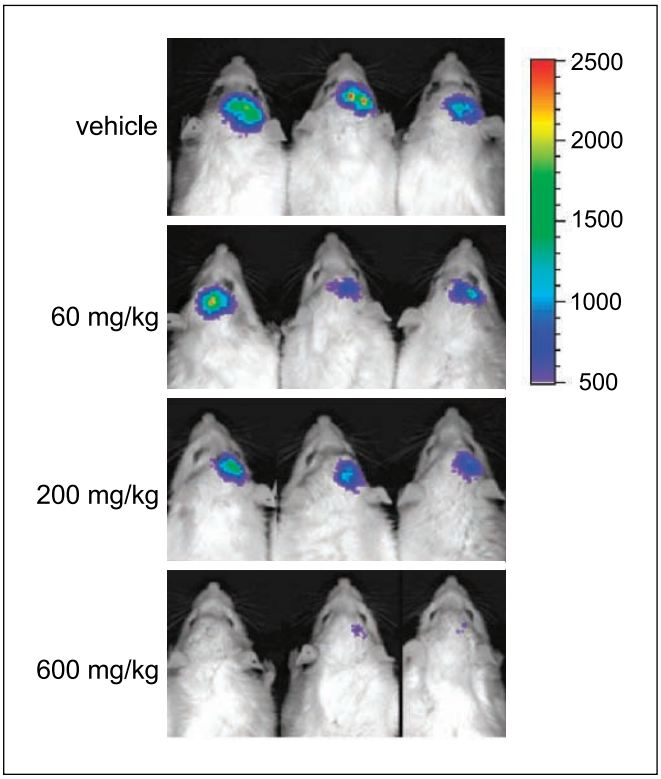


**Figure 3.** BLIs of HIF-1 activity are shown from three representative rats of each group at the end of 2-methoxyestradiol treatment. *Right,* scale of light intensity.

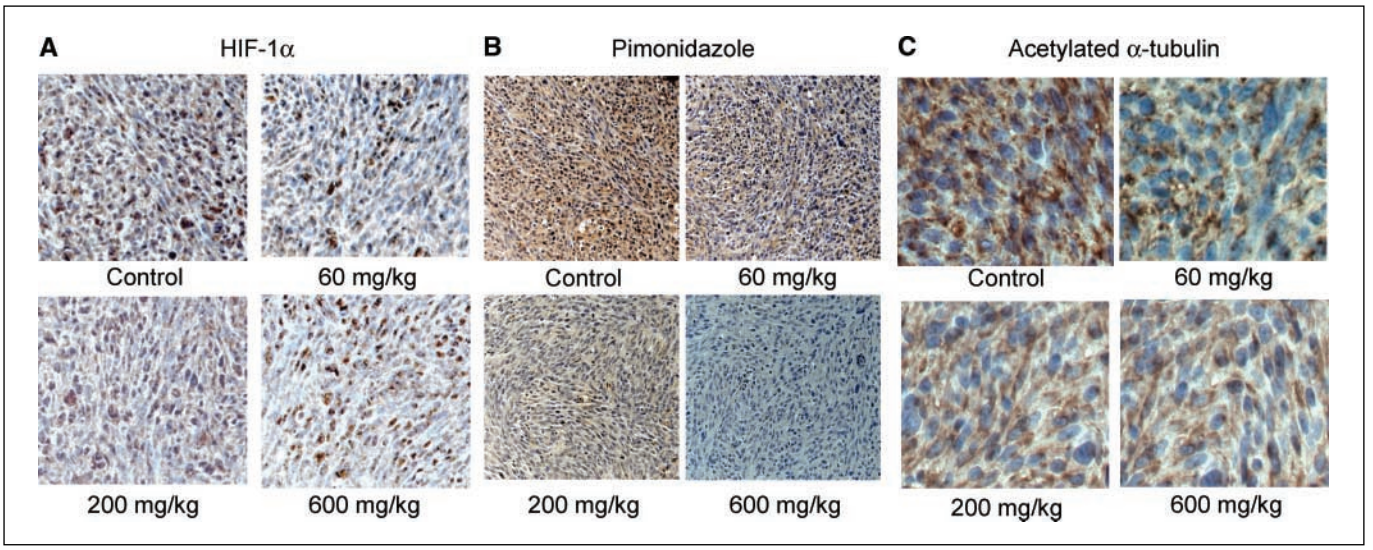


**Figure 4.** Immunohistochemical stainings of HIF-1α (*A*), pimonidazole (*B*), and acetylated α-tubulin (*C*) on a representative tumor tissue section from each group. The semiquantitative analyses of HIF-1α, pimonidazole, and acetylated α-tubulin stainings are summarized in Tables 1 and 2, respectively.

tubulin acetylation, whereas drugs that depolymerize microtubules, such as 2-methoxyestradiol, decrease tubulin acetylation. Therefore, we used tubulin acetylation as a surrogate marker for the effects of 2-methoxyestradiol on microtubule stability. Figure 4*C* shows one representative tumor tissue section per group after 2-methoxyestradiol treatment. Results of immunohistochemistry for acetylated α-tubulin from all samples are summarized in Table 2. There was a dose-dependent reduction of positive staining for acetylated α-tubulin in 2-methoxyestradiol-treated rats, with highly stained areas decreasing from 57% in vehicle-treated animals to 20.0%, 7.4%, and 0% in 60, 200, and 600 mg/kg/d, respectively.

## Discussion

2-Methoxyestradiol, an agent being clinically evaluated as a new anticancer agent, is promising because it preferentially kills cells in hypoxic conditions, unlike other cytotoxic drugs or radiation therapy. The hypoxic tumor environment may enhance the antitumor effect of 2-methoxyestradiol through the ROS-mediated damage to cancer cells, which are already under significant ROS stress caused by hypoxia (27, 28). In addition, 2-methoxyestradiol has been shown to decrease HIF-1α function as a transcriptional factor *in vitro* in a dose-dependent manner (6). However, 2-methoxyestradiol activity had not yet been evaluated *in vivo* in GBM in an orthotopically implanted brain tumor model. Using noninvasive imaging techniques, we measured tumor growth and HIF-1 activity in response to 2-methoxyestradiol treatment in the 9L orthotopic animal model of GBM. Although MRI was used to monitor the tumor volume, BLI was used to monitor the HIF-1 activity using a luciferase vector, whose expression was driven by six HRE motifs. The inhibition of tumor growth in rats with implanted glioma cells occurred in a dose-dependent manner following treatment with 2-methoxyestradiol. We found that the

**Table 1.** Summary of immunostaining of HIF-1α and pimonidazole for all tumor sections

| | − | + | ++ | +++ | Sum | Ratio | *P* |
|---|---|---|---|---|---|---|---|
| HIF-1α | | | | | | | |
| Vehicle | 12.4 ± 3.7 | 23.6 ± 4.1 | 28.5 ± 5.5 | 35.5 ± 3.8 | 1.87 | 1 | |
| 60 mg/kg | 28.0 ± 3.9 | 25.8 ± 4.9 | 22.2 ± 6.2 | 24.0 ± 6.3 | 1.42 | 0.76 | 0.005 |
| 200 mg/kg | 30.0 ± 3.0 | 32.8 ± 4.8 | 19.0 ± 3.5 | 18.2 ± 7.2 | 1.25 | 0.67 | 0.001 |
| 600 mg/kg | 38.1 ± 2.5 | 34.4 ± 9.8 | 15.5 ± 8.8 | 12.0 ± 2.9 | 1.01 | 0.54 | 5e-6 |
| Pimonidazole | | | | | | | |
| Vehicle | 0 | 0 | 13.5 ± 5.5 | 86.5 ± 3.8 | 2.86 | 1 | |
| 60 mg/kg | 10.0 ± 3.0 | 7.8 ± 2.9 | 46.2 ± 11.2 | 36.0 ± 4.1 | 2.08 | 0.73 | 0.008 |
| 200 mg/kg | 0 | 25.0 ± 4.8 | 75.0 ± 3.5 | 0 | 1.75 | 0.61 | 0.002 |
| 600 mg/kg | 11.1 ± 2.5 | 48.4 ± 9.8 | 40.5 ± 10.8 | 0 | 1.29 | 0.45 | 9e-7 |

NOTE: The intensity of HIF-1α and pimonidazole stainings were graded as − (negative), + (weak), ++ (intermediate), and +++ (strong). Percentage of cells in the indicated grade. Sum represents the summation of grade multiplied by the percentage of cells in that grade. For example, the sum for 60 mg/kg HIF-1α dose was calculated as $1 \times 0.258 + 2 \times 0.222 + 3 \times 0.24 = 1.42$. The ratio was obtained by dividing the sum of each grade by the sum of vehicle.

**Table 2.** Summary of immunostaining of acetylated α-tubulin for all tumor sections

| | − | + | ++ | +++ | Sum | Ratio | *P* |
|---|---|---|---|---|---|---|---|
| Vehicle | 0.4 ± 0.3 | 11.2 ± 2.9 | 31.2 ± 5.6 | 57.3 ± 8.7 | 2.34 | 1 | |
| 60 mg/kg | 1.0 ± 0.4 | 38.1 ± 12.1 | 41.0 ± 11.6 | 20.0 ± 3.7 | 1.80 | 0.77 | 0.025 |
| 200 mg/kg | 12.1 ± 0.6 | 37.4 ± 7.7 | 43.1 ± 12.9 | 7.4 ± 2.2 | 1.45 | 0.62 | 0.004 |
| 600 mg/kg | 16.0 ± 4.1 | 69.2 ± 14.8 | 14.8 ± 2.6 | 0 | 0.98 | 0.42 | 2e−5 |

NOTE: The intensity of the staining was graded in the same way as Table 1.

depth of the tumor mass within the brain affected the imaging by BLI, especially in the intermediate dose groups. Components of the tumor closest to the surface were brighter than tumor cells a few millimeters deeper because of the limited penetration depth of scattered light. Thus, the BLI data can only be evaluated in conjunction with MRI to verify that the tumor location is identical between groups in an orthotopic rat brain model. Under such conditions, BLI data are a useful, qualitative measure of HIF-1 activity.

There was a significant inhibition in tumor growth even in the 60 mg/kg/d group accompanied by a dramatic reduction in pimonidazole and HIF-1α staining. Thus, the hypoxic area inside the tumor is decreased by 2-methoxyestradiol as tumor size decreases and tumor oxygenation improves. This reduction in the overall tumor size may reduce the level of hypoxia within the tumor. Alternatively, it is possible that, similar to other antiangiogenic agents (29), a vascular normalization occurs in 2-methoxyestradiol-treated tumors, which could improve blood flow and thus potentially improve results with combined therapies. We postulate that inhibition of tumor growth by the disruption of microtubule formation in actively dividing tumor cells is one of the main mechanisms of action by which 2-methoxyestradiol works in our tumor model. Tubulin acetylation, a post-translational modification that occurs at the conserved lysine residue at position 40 in the $NH_2$ terminus of α-tubulin, has been shown to be decreased by 2-methoxyestradiol in MDA-MB-231 breast cancer cells (30) and in IA9 ovarian cancer cells.[9] As an *in vivo* measurement of 2-methoxyestradiol-mediated microtubule disruption, we compared the extent of microtubule acetylation in the tumor sections (6). Consistent with previous findings, the microtubule deacetylation effect by 2-methoxyestradiol treatment was evident in the treated groups compared with the vehicle-treated group (Table 2), which correlated well with the decrease in tumor growth.

In summary, by using noninvasive imaging techniques, we have measured the changes of tumor size in primary tumors and HIF-1 activity to evaluate the response of 2-methoxyestradiol treatment in an orthotopic animal model of gliomas. The reduction of tumor volume in rats with implanted glioma cells and decreased HIF-1α protein levels, tumor hypoxia, and acetylated tubulin occurred in a dose-dependent manner after treatment with 2-methoxyestradiol. A combination of different imaging modalities may be applicable in the comprehensive *in vivo* monitoring of tumor development and treatment response.

Our results suggest that 2-methoxyestradiol may be a promising chemotherapeutic agent for the treatment of gliomas. This drug is particularly well suited to GBM because of the abundance of neovasculature, and the high expression of HIF-1α is positively associated with the tumor grades in GBM. The demonstration of reduced hypoxia and reduced acetylation in rat tumors may prove useful as biomarkers in future clinical studies. Further preclinical studies are ongoing to assess the effect of low or intermediate doses of 2-methoxyestradiol in combination with chemotherapeutic agents or radiation therapy to guide further clinical studies of this agent in gliomas.

[9] Unpublished data.

## Acknowledgments

Received 4/11/2006; revised 8/29/2006; accepted 9/22/2006.

**Grant support:** Distinguished Cancer Scientist Development Fund of Georgia Cancer Coalition and EntreMed Grant (H. Shim), National Cancer Institute grant 1R01CA114335-01 (P. Giannakakou), and EntreMed, Inc. awards (P. Giannakakou).

The costs of publication of this article were defrayed in part by the payment of page charges. This article must therefore be hereby marked *advertisement* in accordance with 18 U.S.C. Section 1734 solely to indicate this fact.

We thank Dr. Charlie Hao, a Pathologist, for help in evaluating the immunohistochemistry; Adam Marcus for the protocol of tubulin staining and critical review of the article; Ajou University Hospital for supporting the financial expenses for S-H. Kang to carry out this study at Emory University; and Dr. Joann Brooks and Ghazala Datoo for proofreading.

## References

1. Fischer I, Gagner JP, Law M, et al. Angiogenesis in gliomas: biology and molecular pathophysiology. Brain Pathol 2005;15:297–310.
2. Irie N, Matsuo T, Nagata I. Protocol of radiotherapy for glioblastoma according to the expression of HIF-1. Brain Tumor Pathol 2004;21:1–6.
3. Semenza GL, Jiang BH, Leung SW, et al. Hypoxia response elements in the aldolase A, enolase 1 and lactate dehydrogenase A gene promoters contain essential binding sites for hypoxia-inducible factor 1. J Biol Chem 1996;271:32529–37.
4. Semenza GL, Roth PH, Fang HM, et al. Transcriptional regulation of genes encoding glycolytic enzymes by hypoxia-inducible factor 1. J Biol Chem 1994;269:23757–63.
5. Gleadle JM, Ratcliffe PJ. Hypoxia and the regulation of gene expression. Mol Med Today 1998;4:122–9.
6. Mabjeesh NJ, Escuin D, LaVallee TM, et al. 2ME2 inhibits tumor growth and angiogenesis by disrupting microtubules and dysregulating HIF. Cancer Cell 2003;3:363–75.
7. Lis A, Ciesielski MJ, Barone TA, et al. 2-Methoxyestradiol inhibits proliferation of normal and neoplastic glial cells, and induces cell death, *in vitro*. Cancer Lett 2004;213:57–65.
8. Mooberry SL. Mechanism of action of 2-methoxyestradiol: new developments. Drug Resist Updat 2003;6:355–61.
9. Mooberry SL. New insights into 2-methoxyestradiol, a promising antiangiogenic and antitumor agent. Curr Opin Oncol 2003;15:425–30.
10. D'Amato RJ, Lin CM, Flynn E, et al. 2-Methoxyestradiol, an endogenous mammalian metabolite, inhibits tubulin polymerization by interacting at the colchicine site. Proc Natl Acad Sci U S A 1994;91:3964–8.
11. Chamaon K, Stojek J, Kanakis D, et al. Micromolar concentrations of 2-methoxyestradiol kill glioma cells by

an apoptotic mechanism, without destroying their microtubule cytoskeleton. J Neurooncol 2005;72:11–6.
12. Huang P, Feng L, Oldham EA, et al. Superoxide dismutase as a target for the selective killing of cancer cells. Nature 2000;407:390–5.
13. Pelicano H, Feng L, Zhou Y, et al. Inhibition of mitochondrial respiration: a novel strategy to enhance drug-induced apoptosis in human leukemia cells by a reactive oxygen species-mediated mechanism. J Biol Chem 2003;278:37832–9.
14. Pribluda VS, Gubish ER, Jr., Lavallee TM, et al. 2-Methoxyestradiol: an endogenous antiangiogenic and antiproliferative drug candidate. Cancer Metastasis Rev 2000;19:173–9.
15. Post DE, Van Meir EG. Generation of bidirectional hypoxia/HIF-responsive expression vectors to target gene expression to hypoxic cells. Gene Ther 2001;8: 1801–7.
16. Barker M, Hoshino T, Gurcay O, et al. Development of an animal brain tumor model and its response to therapy with 1,3-bis(2-chloroethyl)-1-nitrosourea. Cancer Res 1973;33:976–86.
17. Sahin B, Aslan H, Unal B, et al. Brain volumes of the lamb, rat, and bird do not show hemispheric asymmetry. Image Anal Stereol 2001;20:9–13.
18. Bos R, Zhong H, Hanrahan CF, et al. Levels of hypoxia-inducible factor-1 alpha during breast carcinogenesis. J Natl Cancer Inst 2001;93:309–14.
19. Cappuzzo F, Hirsch FR, Rossi E, et al. Epidermal growth factor receptor gene and protein and gefitinib sensitivity in non-small-cell lung cancer. J Natl Cancer Inst 2005;97:643–55.
20. Rijken PF, Peters JP, Van der Kogel AJ. Quantitative analysis of varying profiles of hypoxia in relation to functional vessels in different human glioma xenograft lines. Radiat Res 2002;157:626–32.
21. Rofstad EK, Halsor EF. Hypoxia-associated spontaneous pulmonary metastasis in human melanoma xenografts: involvement of microvascular hot spots induced in hypoxic foci by interleukin 8. Br J Cancer 2002;86:301–8.
22. Lee YM, Jeong CH, Koo SY, et al. Determination of hypoxic region by hypoxia marker in developing mouse embryos *in vivo*: a possible signal for vessel development. Dev Dyn 2001;220:175–86.
23. Ljungkvist AS, Bussink J, Rijken PF, et al. Changes in tumor hypoxia measured with a double hypoxic marker technique. Int J Radiat Oncol Biol Phys 2000;48:1529–38.
24. Escuin D, Kline ER, Giannakakou P. Both microtubule-stabilizing and microtubule-destabilizing drugs inhibit hypoxia-inducible factor-1alpha accumulation and activity by disrupting microtubule function. Cancer Res 2005;65:9021–8.
25. L'Hernault SW, Rosenbaum JL. Chlamydomonas alpha-tubulin is posttranslationally modified by acetylation on the epsilon-amino group of a lysine. Biochemistry 1985;24:473–8.
26. Sasse R, Gull K. Tubulin post-translational modifications and the construction of microtubular organelles in *Trypanosoma brucei*. J Cell Sci 1988;90:577–89.
27. Chandel NS, Maltepe E, Goldwasser E, et al. Mitochondrial reactive oxygen species trigger hypoxia-induced transcription. Proc Natl Acad Sci U S A 1998;95: 11715–20.
28. Mansfield KD, Simon MC, Keith B. Hypoxic reduction in cellular glutathione levels requires mitochondrial reactive oxygen species. J Appl Physiol 2004;97:1358–66.
29. Jain RK. Tumor angiogenesis and accessibility: role of vascular endothelial growth factor. Semin Oncol 2002; 29:3–9.
30. Gokmen-Polar Y, Escuin D, Walls CD, et al. β-Tubulin mutations are associated with resistance to 2-methoxyestradiol in MDA-MB-435 cancer cells. Cancer Res 2005;65:9406–14.